Advanced Composites and Hybrid Materials (2024) 7:45
https://doi.org/10.1007/s42114-024-00859-w

RESEARCH

Investigating the effects of γ-ray irradiation on the mechanical and dielectric properties of poly(lactide)/poly(butylene adipate-*co*-terephthalate)/carbon nanotubes composites

Yiyang Zhou[1,2] · Ming Chen[2,3] · Xinwen Xu[2,3] · Qiuyue Meng[2,3] · Jiaying Tu[2,3] · Chenyu Ma[2,3] · Pei Xu[2,3] · Ping Wang[1] · Yunsheng Ding[2,3]

Received: 8 August 2023 / Revised: 29 January 2024 / Accepted: 14 February 2024 / Published online: 28 February 2024

Abstract
Poly(lactide)/poly(butylene adipate-*co*-terephthalate)/carbon nanotubes (PLA/PBAT/CNTs) composites with a fixed composition were prepared by melt blending without strict control of the pretreatment of CNTs. Then, γ-ray irradiation was utilized to control microstructure, enhance component-interaction, and improve the performance of the prepared PLA/PBAT/CNTs composites, and the effects of different doses of γ-ray irradiation on mechanical and dielectric properties of the composites were investigated. Mechanical test results reveal that the irradiated PLA/PBAT/CNTs composites exhibit much better mechanical properties than the unirradiated composites. Especially when the irradiation dose is 6 kGy, the tensile strength of the composites increases from 31.9 to 42.1 MPa; meanwhile, the elongation at break increases from 160 to 230%. Dielectric test results indicate that when the irradiation dose reaches 24 kGy, the dielectric constant of the composites is significantly enhanced and the dielectric loss is obviously decreased. The rheology tests reveal the irradiated PLA/PBAT/CNTs composites display a significant increase in the storage modulus compared to unirradiated composites, which suggests that the γ-ray irradiation can induce the formation of crosslinking network in the polymer matrix; meanwhile, the interaction force between CNTs and polymer matrix is enhanced in the composites. The significant morphological changes observed in the SEM micrographs can be consistence with the rheology test results. This work provides a facile way for constructing high-performance PLA blend composites, which can be applied in electronic fields.

Keywords Poly(lactide) · Carbon nanotubes · Composites · Mechanical properties · Dielectric properties · γ-ray irradiation

1 Introduction

Polymer composite dielectrics have attracted numerous attention for outstanding flexibility, easy-to-process, and lightweight compared with ceramic materials, and they are considered the ideal choice for many power electronics, power conditioning, and pulsed power applications [1–7]. Yet, most of petroleum-based polymer is difficult to degrade. The waste electrical equipment based on polymer composite dielectrics can lead to "white pollution." Poly(lactide) (PLA) is a biodegradable polymer synthesized by ring-opening polymerization of lactide, which can be derived from renewable sources such as corn, and PLA has been regarded as one of the most promising polymer matrix for polymer composite dielectrics owing to its excellent biodegradability, renewability, high strength, and easy processibility [8–10].

However, the poor dielectric properties of PLA restrict its application in dielectric materials. Blending PLA with particles which have excellent electrical properties is an effective way to improve the dielectric properties. The specific functional fillers, such as some carbon materials and transition metal oxides, exhibit good electrical properties [11–15]. Among the functional particles, carbon nanotubes

✉ Ping Wang
anjzwp@ahjzu.edu.cn

✉ Yunsheng Ding
dingys@hfut.edu.cn

[1] Anhui Province International Research Center On Advanced Building Materials, School of Materials and Chemical Engineering, Anhui Jianzhu University, Hefei 230601, China

[2] School of Chemistry and Chemical Engineering, Hefei University of Technology, Hefei 230009, China

[3] Anhui Key Laboratory of Advanced Functional Materials and Devices, Hefei 230009, China

(CNTs) have excellent thermal, electrical, and mechanical properties; hence, CNTs as conductive fillers are increasingly used to improve the dielectric properties of PLA composites [16–18]. The mechanical and dielectric properties of PLA composites containing CNTs are strongly dependent on the CNTs-polymer interactions and the dispersion of CNTs in polymer matrix, but it has been reported that usually at the interface between the CNTs and the polymer, there is just a van der Waals interaction that is able to produce only a weak normal forces and almost null shear strength [19]. In order to improve the CNTs-polymer interactions and refine the dispersion of CNTs in polymer matrix, various attempts have been made. Surface functionalization of CNTs is an effective way to improve the interaction between CNTs and polymer matrix. Raja et al. introduced UV/ozone-modified carbon nanotubes into polyurethane (PU)/PLA blends, and it was found that the composites containing modified CNTs exhibit better properties compared to the pristine CNTs loaded system, which is attributed to the higher polymer-CNTs interactions and the fine dispersion of the modified CNTs in the matrix [20]. Seligra et al. prepared PLA-based nanocomposites reinforced by Fenton reaction CNTs, and the excellent dispersion of the fillers in the PLA matrix was observed [21]. Sun and He synthesized CNT-*g*-poly(D-lactide) via ring-opening polymerization initiated by modified CNTs, and the results indicated that stereocomplex crystallites can be formed between the PLA matrix and CNT-*g*-poly(D-lactide), which leads to the strong covalent/stereocomplex CNT-matrix interactions and well dispersion of CNTs [22].

On the other hand, the brittleness of PLA also restricts its application in dielectric materials. Blending PLA with flexible biodegradable polymers such as poly(butylene adipate-*co*-terephthalate) (PBAT), polycaprolactone (PCL), and polybutylene succinate (PBS) is efficient in improving the toughness of PLA [23–26]. PLA/PBAT blends are highly promising materials due to the considerable mechanical strength and the extreme toughness, but the PLA/PBAT blends are thermodynamically immiscible owing to their low interfacial adhesion, and the compatibility of PLA and PBAT is the key technical point to be addressed in order to obtain materials with excellent performance. Incorporating compatibilizers into the PLA/PBAT blends can improve the phase interface affinity of PLA and PBAT, and the compatibilizers can be mainly divided into two types that include physical compatibilizer and reactive compatibilizer.

The physical compatibilizers are commonly block copolymers or graft copolymers that can emulsify the phase interface to improve the interfacial adhesion of PLA/PBAT blends. Wang et al. investigated the effect of the chain length of PLA-PBAT-PLA tri-block copolymers on the compatibilization of PLA/PBAT blends, and the results showed that the tri-block copolymer with long-chain PLA blocks achieved more effective compatibilization of PLA and PBAT compared to the short-chain PLA blocks [27]. Reactive compatibilizers can form a chemical bonding between the PLA and PBAT, thus enhancing the interfacial adhesion between the polymer phases. Wang et al. employed a multifunctional epoxy oligomer (ADR) as a reactive compatibilizer for improving the compatibility of PLA and PBAT, and it was revealed that ADR can induce the in situ formation of PLA-*g*-PBAT-branched copolymers and enhance the compatibility between PLA and PBAT [28]. Han et al. used environmentally friendly epoxidized soybean oil (ESO) to improve the compatibility of PLA and PBAT, and the results indicated that the ESO could react with PLA and PBAT to form a chemical bonding interface [29].

Although the pretreatment of CNTs and the introduction of compatibilizers are demonstrated to be important in improving the interaction between PLA and PBAT in PLA/PBAT blends or the interactions between CNTs and PLA in PLA/CNTs composites, to evaluate a facile way to realize the simultaneously effective control of the polymer–polymer interaction and CNTs-polymer interactions microstructure of PLA/PBAT/CNTs composites is still a challenge.

When exposed to the irradiation of high energy rays, free radicals can be formed inside the polymer matrix, and they may couple with each other to form covalent bonds, which is helpful in enhancing the interfacial adhesion between the polymer components [30, 31]. Jeon et al. blended poly(ε-caprolactone) (PCL) into PLA and compatibilized the PLA/PCL blends by electron-beam irradiation in the presence of glycidyl methacrylate (GMA), and the results showed that the electron-beam irradiation can induce the occurrence of cross-copolymerization at the PLA/PCL interface in the presence of GMA, which will lead to the improvement of interfacial adhesion in PLA/PCL blends [32]. Meanwhile, it has been reported that high energy ray irradiation has the potential to enhance the interaction force between nanofiller and polymer matrix. Tarawneh et al. prepared PLA-based thermoplastic elastomer containing CNTs and montmorillonite nanoclay, and the results indicated that γ-ray irradiation promoted better interactions and improved the compatibility between the nanofiller and TPE [33].

However, according to our knowledge, there are few works utilizing γ-ray irradiation to control the microstructure and properties of PLA/PBAT/CNTs composites. In this work, we focus on whether the γ-ray irradiation can lead to the in situ enhancement of the component interaction in the composites. An epoxy chain extender (ADR) was introduced into the composites in order to improve the processing stability of PLA and PBAT during melting blending. Trimethylolpropane trimethacrylate (TMPTMA), an irradiation sensitizer, was incorporated into the system for the in situ formation of the crosslink network inside composites during γ-ray irradiation. The effects of γ-ray irradiation on

component interaction, mechanical, and dielectric properties of PLA/PBAT/CNTs composites were investigated.

2 Experimental section

2.1 Materials

PLA (4032D) was procured from Nature Works LLC, the USA, which possesses a weight average molecular mass (M_w) of 195,000 g/mol. PBAT (FBX 7011) was provided from BASF Corporation, Germany, which possesses a M_w of 40,000 g/mol. ADR (4468) was obtained from BASF Corporation, Germany, with a M_w of 7250 g/mol and an epoxy equivalent of 310 g/mol. CNTs with a 10–20-nm outer diameter ranger and 10–30-μm length ranger were purchased by Nanjing XFNANO Material Technology Co., Ltd., with a purity of over 95%. TMPTMA was provided from KPX Green Chemical Co., Ltd.

2.2 Sample preparation

The PLA/PBAT/CNTs composites were prepared using a melt compounding process employing HAPRO rheometer (RM-200C) at 180 °C and 50 rpm. The CNTs, TMPTMA, and ADR contents are fixed at 4 wt%, 3 wt%, and 2 wt%, and the composite had a PLA:PBAT composition of 70:30. The melt-blended composites were put into a vacuum flatbed vulcanizing machine and hot-pressed at 180 °C and 5 MPa.

2.3 Irradiation conditions

The samples were irradiated in vacuum at ambient conditions with a ^{60}Co γ source at the University of Science and Technology of China, Hefei, China, at an average dose rate of approximately 3 kGy/h. Target doses of 0, 6, 12, and 24 kGy were applied. The sample preparation process is shown in Fig. S1.

2.4 Characterization

The tensile properties of the PLA/PBAT/CNTs composites were investigated by using an electrical universal testing machine (CMT4304, MTS) according to the ISO 527–3 standards. The dielectric permittivity was measured using an Agilent E4980A LCR meter at a temperature of 30 °C. The rheological behavior of the composites was obtained by a rotating rheometer (DHR-1, TA, USA) with a parallel plate geometry of 25 mm in diameter and a gap of 0.9 mm at 180 °C. The morphologies of the cryofracture surfaces of PLA/PBAT/CNTs composites were observed by using a SU-8020 field emission scanning electron microscopy (FESEM; Hitachi, Japan) at 5 kV. The atomic force microscopy (AFM) measurements were carried out using tapping mode on a Dimension ICON AFM (Bruker, USA), and AFM pictures of the cryofracture surfaces were collected in the air temperature without any extra preparation. A Talos F200X G2 high-resolution transmission electron microscopy (HRTEM; Thermo Fisher Scientific, USA) was also employed to observe the structure of the composites. The nonisothermal crystallization behavior was performed by DSC (TA Q2000). The samples were firstly heated from 40 to 200 °C and maintained for 5 min to eliminate thermal history, then cooled down to − 60 °C at a rate of 10 °C/min, and heated to 200 °C again. Thermal gravimetric analysis (TGA) was conducted to determine the thermal stability of the composites under nitrogen atmosphere. A TA Q500 model TGA instrument was employed, and samples were heated from room temperature to 600 °C at a heating rate of 10 °C/min. The dynamic mechanical analysis (DMA) test was performed from 30 to 140 °C at a heating rate of 3 °C/min and frequency of 1 Hz by using the DMA Q800 (TA, USA).

3 Results and discussion

3.1 Mechanical properties, dielectric behavior, and rheological behavior of the composites

Figure 1a, b shows the mechanical properties of PLA/PBAT/CNTs composites with different γ-ray irradiation doses. The unirradiated PLA/PBAT/CNTs composites exhibit a tensile strength of about 31.9 MPa and an elongation at break of about 160%. When the irradiation is 6 kGy, the tensile strength of the composites reaches about 42.1 MPa, and the elongation at break of the composites reaches about 230%, which suggests that the mechanical properties of PLA/PBAT/CNTs composite can be significantly improved after receiving a low dose of γ-ray irradiation. As the irradiation dose further increases, tensile strength of the composites is not obviously improved, but the elongation at break of the composites is decreased. It may be because that when the irradiation dose is further increased, the formation of more crosslinking network inside composites owing to the radical reactions induced by γ-ray can hinder the movement of polymer chain. Meanwhile, chain scission reactions can also occur inside the crosslinking network; thus, the elongation at break of the composites is decreased [34–36].

The dielectric constant (ε') and dielectric loss (*Tan* δ) of the PLA/PBAT/CNTs composites are presented in Fig. 1c, d, individually. Compared to the unirradiated samples, the ε' of the composites increases slightly when the irradiation dose is 6 kGy, but the *Tan* δ decreases significantly. Above phenomenon can be related to the enhancement of the polymer-CNTs interaction. As discussed before, when under γ-ray irradiation, the radicals can be formed in the composites, and the

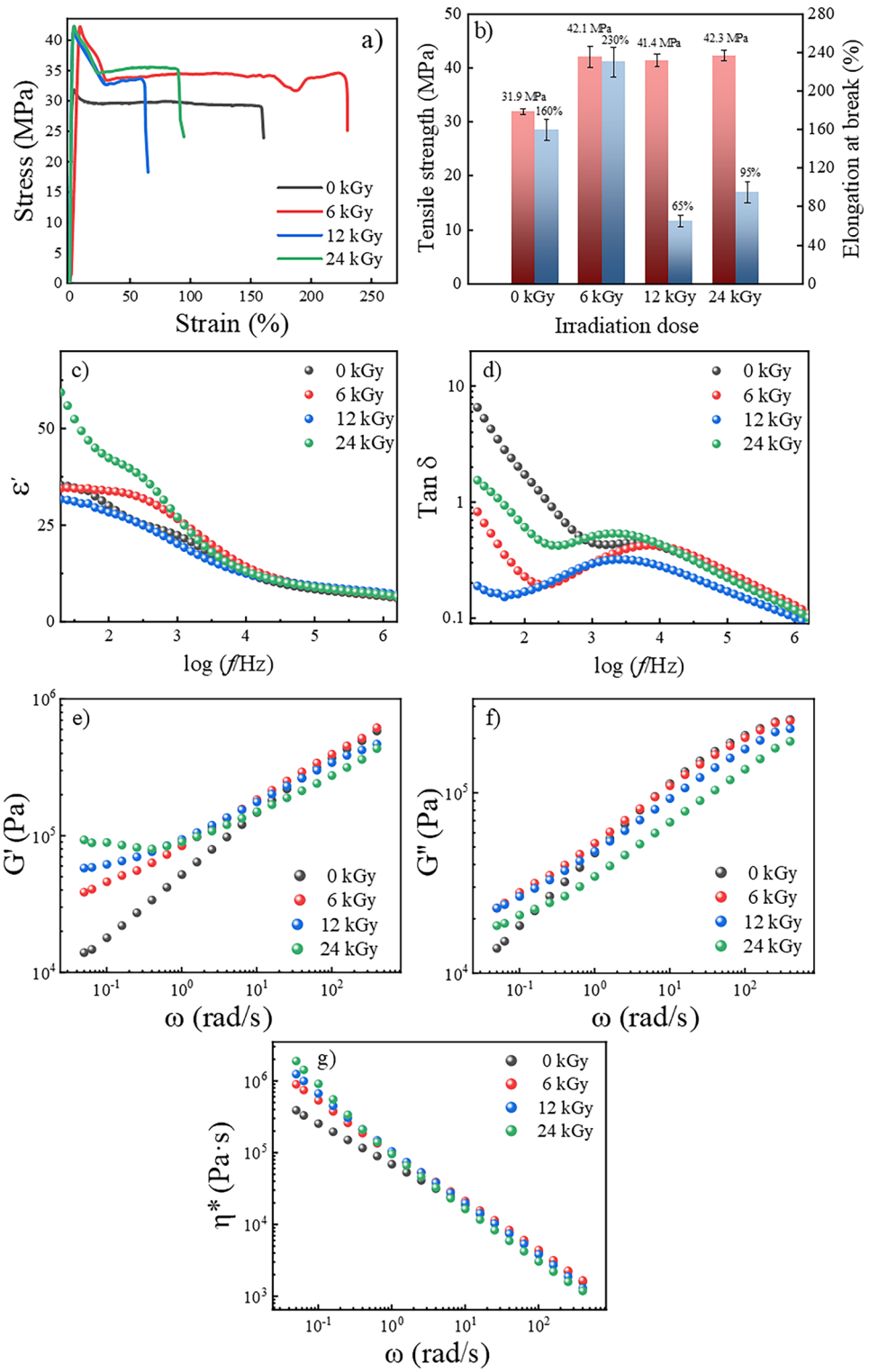

Fig. 1 Mechanical properties, dielectric behavior, and rheological behavior of PLA/PBAT/CNTs composites with different irradiation dose: **a**, **b** stress–strain curve and mechanical parameters; **c**, **d** dielectric behaviors; **e**, **f**, **g** rheological behavior

CNTs can trap the generated radicals, leading to the increase in the interaction between polymer matrix and CNTs. The adjacent CNTs can act as electrodes, and the polymer can act as a dielectric to assemble the microcapacitor, which greatly increases the interfacial polarization and enhances the ε' [37–40]. In addition, the enhanced interaction between the matrix and the filler can effectively reduce the *Tan δ*. When the irradiation dose further increases to 12 kGy, the ε' and *Tan δ* decrease compared to the composite with an irradiation dose of 6 kGy. It is because when the irradiation

dose increases, the chain segment motion of the polymer matrix is also inhibited owing to the more densely crosslinking networks in the polymer matrix; thus, the *Tan δ* of the composites is reduced. Moreover, the structural change of CNTs may lead to the change in the interfacial structure between polymer matrix and CNTs, resulting in the reduced interfacial polarization; hence, the ε' of the composites is decreased. Interestingly, when the irradiation dose reaches 24 kGy, the ε' of the composites increases significantly, while the *Tan δ* remains lower than that of the unirradiated samples. It is possible that high-dose irradiation can further change the interfacial structure between CNTs and polymer matrix [41]. Meanwhile, further aggravation of chain scission reactions can increase the molecular dipole orientation [42]. The smaller molecular size increases the number of interfaces per unit volume, which favors an increase in interfacial polarization, leading to an increase in the ε' [43–46]. According to rheological results, a three-dimensional network of CNTs is formed when the irradiation dose reaches 24 kGy, indicating the formation of a conductive pathway, which causes an increase in leakage current, and ultimately a relatively high *Tan δ* compared to the irradiated sample [37, 47–49]. Overall, γ-ray irradiation has a strong effect on the interfacial structure between CNTs and polymer matrix, which leads to charge accumulation and induces interfacial polarization, resulting in lower *Tan δ* [43, 50].

Figure 1e–g displays the storage modulus (G'), loss modulus (G''), and complex viscosity (η^*) of unirradiated and irradiated PLA/PBAT/CNTs composites, respectively. It should be pointed out that when the irradiation dose reached 24 kGy, a clear platform appeared in the low frequency region according to the curves of G' of PLA/PBAT/CNTs composites with scanning angular frequency versus the logarithm of sweep frequencies, and G' is not sensitive to the change in frequency, indicating that the motion of long-range polymer chains is significantly restricted [51]. The significant restriction of the motion of polymer chain is owing to the formation of the crosslinking network inside polymer matrix and the enhancement of the interaction between polymer matrix and CNTs. The G'' of the composites is also significantly decreased compared to other irradiated samples. It is because the solid network of CNTs in the polymer matrix is more stable when the irradiation dose reaches 24 kGy; thus, the internal energy dissipation of the filler/polymer interphase is decreased [52–54]. According to mechanical properties and dielectric behavior, it may be assumed that when the irradiation dose is 24 kGy, the optimized interfacial structure between the polymer matrix and CNTs is obtained, although the structural change of the crosslinking network inside polymer matrix can weaken the mechanical properties of the composites.

In conclusion, the γ-ray irradiation has a strong effect on the mechanical properties, dielectric behavior, and rheological behavior of the composites, which might be attributed to the enhancement of the CNTs-polymer interactions and polymer–polymer interactions induced by the irradiation.

3.2 Morphological analysis of the composites

The SEM, AFM, and TEM micrographs of cryogenically fractured surfaces of PLA/PBAT/CNTs composites are presented in Fig. 2. As can be observed from the SEM micrographs, compared to the unirradiated composites, the irradiated composites show a rough fracture surface over the entire micrographs. Moreover, more CNTs are pulled out from the polymer matrix with the increase of irradiation dose. The roughness observed for the fractured surface of the irradiated samples could evidence vigorous interfacial interactions between PLA and PBAT phases. Meanwhile, AFM micrographs suggest that the phase structure of the composites is significantly changed after irradiation. When the composites are under irradiation, macromolecular radicals can be formed in the polymer matrix; they can couple with each other to form a crosslinking network structure. The reactions between PLA macromolecular radicals and PBAT macromolecular radicals can enhance the interaction between PLA and PBAT, especially the TMPTMA located at the interface between two polymer phases can promote the crosslinking reactions between PLA and PBAT chains, which can further improve the compatibility of two polymers [55]. Thus, the phase structure of the composites and the interaction between the polymer matrixes are obviously changed after irradiation. On the other hand, since the CNTs can act as a radical scavenger and anchor radicals on CNTs, the interaction between CNTs and polymer matrix can also be improved after irradiation [56]. Take consideration that CNTs tend to migrate into the low-viscosity PBAT phase, the covalent interactions between CNTs and PBAT macromolecular radicals may play a dominant role in the composites [57]. Owing to the simultaneously enhancement of the polymer–polymer interaction and polymer-CNTs interaction, the microstructure of the PLA/PBAT/CNTs composites is significantly changed after irradiation. It should be mentioned that the structure of CNTs is not significantly changed after irradiation according to the TEM micrographs; hence, the enhancement of the mechanical and dielectric properties of the composites is mainly due to the change in the polymer–polymer interactions and polymer-CNTs interactions under irradiation.

3.3 Nonisothermal crystallization behavior and thermal stability of the composites

The DSC and TG curves of the unirradiated and irradiated composites are exhibited in Fig. 3, and the relevant parameters are listed in Tables 1 and 2. The results show the γ-ray irradiation has a significant influence on the crystallization behavior of the PLA/PBAT/CNTs composites. As can be seen in Fig. 3a,

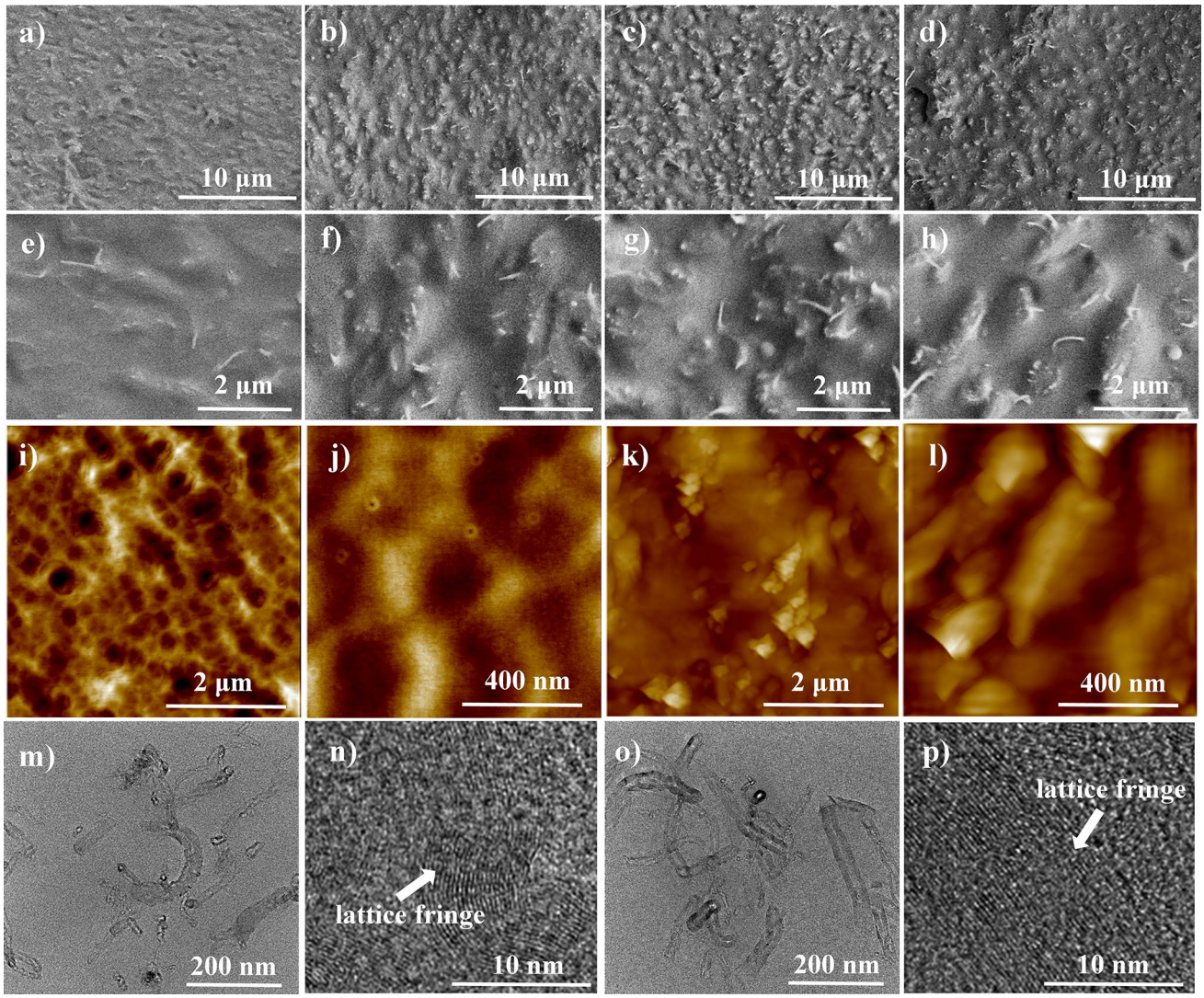

Fig. 2 SEM, AFM, and TEM micrographs of PLA/PBAT/CNTs composites with different irradiation doses: **a**, **e** SEM images (0 kGy); **b**, **f** SEM images (6 kGy); **c**, **g** SEM images (12 kGy); **d**, **h** SEM images (24 kGy); **i**, **j** AFM image (0 kGy); **k**, **l** AFM image (24 kGy); **m**, **n** TEM image (0 kGy); **o**, **p** TEM image (24 kGy)

PLA does not exhibit any crystallization peak during the cooling process. The cold crystallization temperature (T_{cc}) of irradiated samples is all increased during the secondary heating process in Fig. 3b, while the melting point (T_m) of PLA is also decreased. It is because the formation of crosslink network can restrict the PLA chain segment motion for crystallization, so that PLA segments are hard to stack regularly, and the T_{cc} of the PLA is increased. On the other hand, imperfect crystallites are formed inside the composites after irradiation because the crosslinking network interferes with the crystallization process; hence, the T_m of the PLA is decreased [58–60]. It should be mentioned that although the crystallization ability of PLA is weakened, the glass transition temperature of PLA is significantly enhanced, which is benefit for the improvement of the thermal stability of the composites [61].

The residual mass of the composites after thermal decomposition can be used to characterize the actual amounts of inorganic fillers added. As can be seen in the TG curves, the residual mass of all composites is essentially the same at 6%, indicating the presence of residual carbon formed by polymer cracking in addition to CNTs [62–64]. On the other hand, there is a slight drop in the mass of the composite around 200–300 °C for unirradiated composite, which may correspond to the decomposition of TMPTMA. After irradiation, the slight drop in mass disappears; it is because that the covalent bond is formed between TMPTMA and polymer chains inside composites owing to the irradiation-induced radical reactions, which improve the thermal stability of TMPTMA. As the irradiation dose increases, the thermal stability of the composites does not significantly

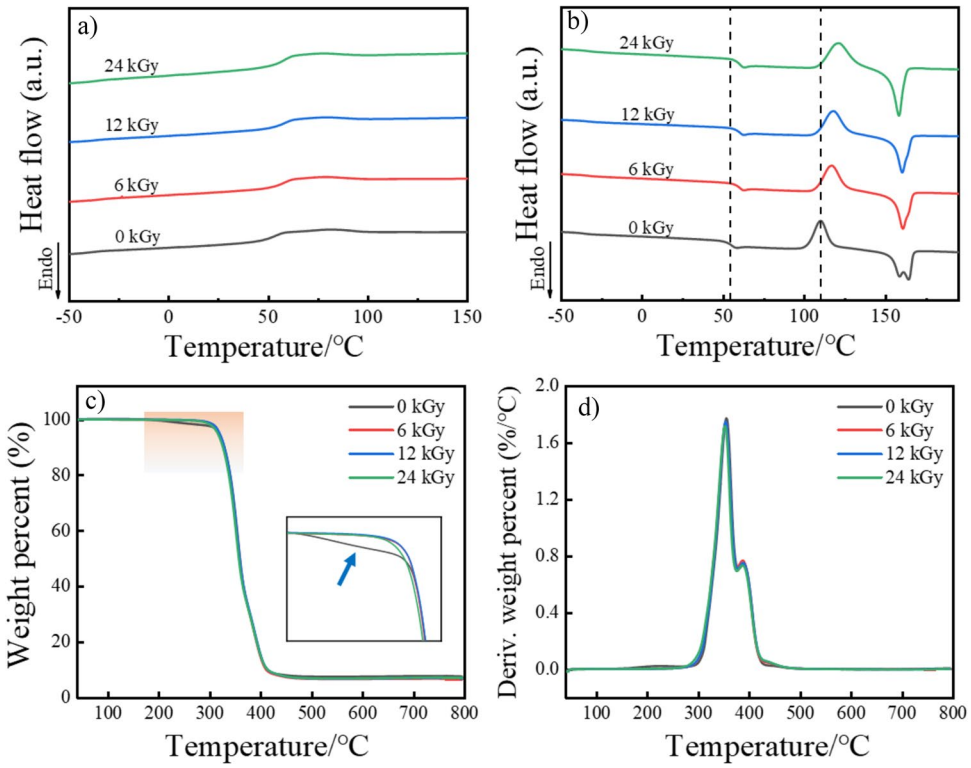

Fig. 3 Nonisothermal crystallization behavior and thermal stability of PLA/PBAT/CNTs composites with different irradiation dose: **a**, **b** DSC curves; **c** TG curves; **d** DTG curves

Table 1 Thermal characteristics data from DSC analysis of PLA/PBAT/CNTs composites with different irradiation doses

Irradiation dose (kGy)	T_g (°C)	T_c (°C)	H_{cc} (J/g)	T_m (°C)	H_m (J/g)	X_c (%)
0	55.3	109.5	16.9	158.5/164.2	19.5	4.4
6	60.2	116.5	17.8	160.6	18.6	1.3
12	60.0	117.3	18.3	160.3	18.9	1.0
24	60.3	120.6	22.7	158.2	23.7	1.7

change. Although the formation of crosslinked polymer network inside composites induced by irradiation is helpful for the improvement of thermal stability of the composites, the concurrent chain scission reactions can also weaken the thermal stability of the composites; hence, the thermal stability of the samples is not obviously improved [65–67].

3.4 Dynamic mechanical analysis of the composites

Temperature dependence of storage modulus and loss factor (*Tan δ*) for the composites with different irradiation dose are shown in Fig. 4. The storage modulus of the composites is obviously increased and then decreased during irradiation. On the other hand, all irradiated composites exhibit higher glass transition temperature determined for the maximum of the loss factor. Above phenomenon also indicates the enhancement of the CNTs-polymer interactions, and polymer–polymer interactions inside composites induced by irradiation can significantly restrict the movement of PLA and PBAT chains, which is consistence with the DSC and rheological results. When the irradiation dose reaches 24 kGy, the storage modulus of the composites is decreased; it may be because that the free chains formed at higher irradiation dose can improve the mobility of PLA and PBAT chains.

In summary, high performance PLA/PBAT/CNTs composites are obtained when exposed to the γ-ray. The structural evolution of the composites under irradiation is

Table 2 Thermal stabilities characterization date of PLA/PBAT/CNTs composites with different irradiation doses

Irradiation dose (kGy)	$T_{5\%}$ (°C)	$T_{50\%}$ (°C)	T_{max1} (°C)	T_{max2} (°C)
0	318.4	359.3	355.8	394.3
6	318.7	358.1	354.3	391.3
12	319.3	358.8	353.3	389.8
24	315.4	356.9	351.8	393.0

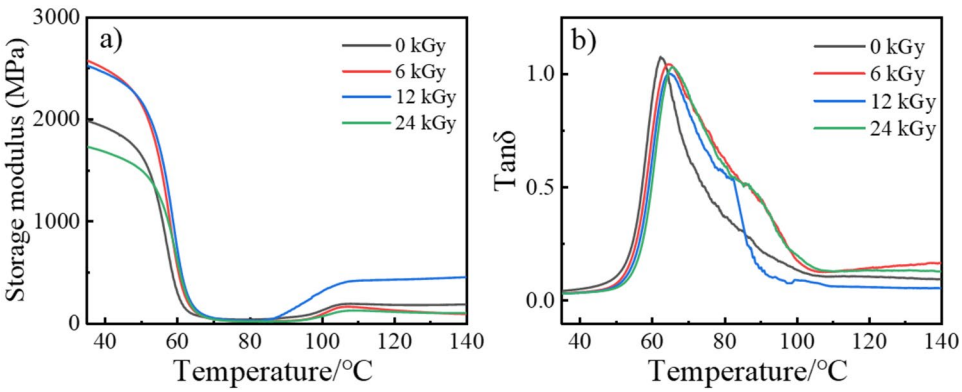

Fig. 4 DMA curves of PLA/PBAT/CNTs composites with different irradiation doses: **a** temperature dependence of storage modulus, **b** temperature dependence of tan δ

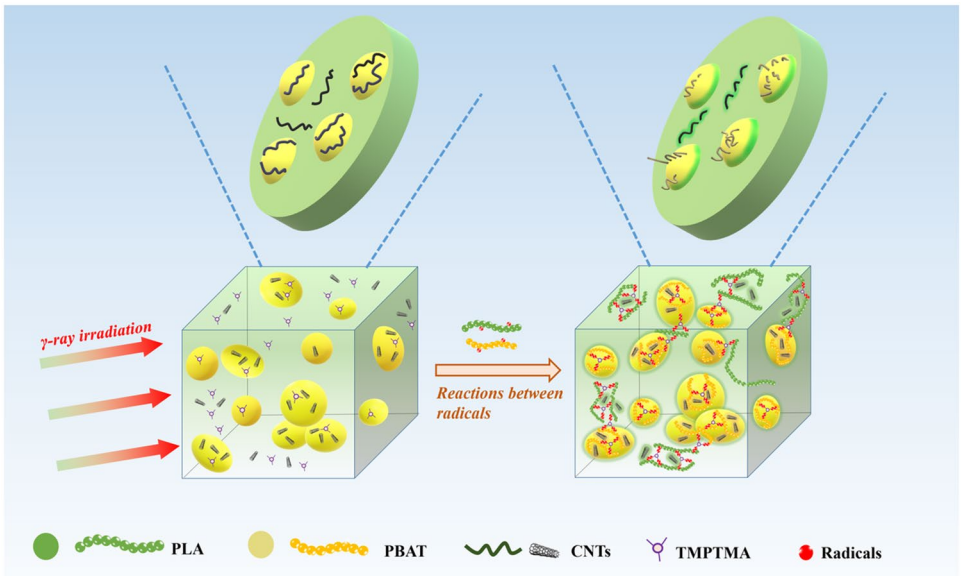

Fig. 5 The structural evolution of the PLA/PBAT/CNTs composites under γ-ray irradiation

illustrated in Fig. 5. After irradiation, PLA and PBAT macromolecular radicals can be formed in the composites, and the reactions between PLA macromolecular radicals and PBAT macromolecular radicals can enhance the interaction between PLA and PBAT. The TMPTMA located at the interface can promote the crosslinking reactions between PLA and PBAT chains, thus further improve the interfacial adhesion between PLA and PBAT. Meanwhile, the TMPTMA can also facilitate the crosslinking process of PLA or PBAT, which is beneficial for the improvement of the mechanical properties of the composites. The interaction between CNTs and polymer matrix can be also improved after irradiation. Although CNTs tend to migrate into the low-viscosity PBAT phase and the irradiation may not significantly change the dispersion of CNTs in the polymer matrix, the simultaneously enhancement of the polymer–polymer interaction and polymer-CNTs interaction can obviously improve the properties of PLA/PBAT/CNTs composites, especially the change in interaction between polymer matrix and CNTs has a strong impact on the dielectric properties of the composites.

4 Conclusion

PLA/PBAT/CNTs composites with excellent mechanical and dielectric properties were prepared without strict control of the pretreatment of CNTs, because the in situ enhancement of component interaction in the composites could be realized when the composites are exposed to γ-ray irradiation. The microstructure and properties of the composites can be effective controlled by simply adjusting the irradiation dose. When the irradiation dose is 6 kGy, the tensile strength of the composites increases from 31.9 to 42.1 MPa, and the elongation at break increases from 160 to 230% compared to unirradiated composites. As the irradiation dose reaches 24 kGy, the dielectric constant of the composites is significantly enhanced, and the dielectric loss is obviously

decreased; meanwhile, the composites also possess good rigidity-toughness balance. The formation of crosslinking network and the enhancement of interaction force between CNTs and polymer matrix in the nanocomposites are proved by rheology tests, and SEM micrographs indicate the morphology of the composites is significantly changed with the γ-ray irradiation. In summary, this work provides a facile way to construct high-performance PLA blend composites without the pretreatment of CNTs, which can be applied in electronic fields.

Supplementary Information The online version contains supplementary material available at https://doi.org/10.1007/s42114-024-00859-w.

Author contribution Ping Wang and Yunsheng Ding designed the research and led the study. Yiyang Zhou designed and produced the samples. Yiyang Zhou, Ming Chen, Xinwen Xu, Qiuyue Meng, Ping Wang, and Yunsheng Ding investigated the mechanical properties, dielectric behavior, and rheological behavior of the composites. Yiyang Zhou, Jiaying Tu, Chenyu Ma, Pei Xu, Ping Wang, and Yunsheng Ding conducted the SEM, AFM, TEM, and other tests of the composites. Yiyang Zhou, Ping Wang, and Yunsheng Ding wrote the manuscript. All authors have given approval for the final version of the manuscript.

Funding This research was supported by the National Natural Science Foundation of China (grant No. U2001223 and No. 51903002), the Major Science and Technology Special Projects in Anhui Province (No. 2021e03020008 and No. 202203c08020009), Excellent Youth Projects of Anhui Provincial Natural Science Foundation (No. 2308085Y34), University Natural Science Outstanding Youth Research Projects of Anhui Province (No. 2022AH020024), University Major Research Projects in Philosophy and Social Sciences of Anhui Province (No. 2022AH040047), Major Science and Technology Projects of Anhui Province (No. 202103a05020031), Wuhu Key Technology Major R&D Projects (No. 2022yf27), and the University Synergy Innovation Program of Anhui Province (No. GXXT -2023-098).

Data availability The data that support the findings of this study are available from the corresponding authors upon reasonable request.

Declarations

Competing interests The authors declare no competing interests.

References

1. Hassan YA, Hu H (2020) Current status of polymer nanocomposite dielectrics for high-temperature applications. Compos A 138:106064. https://doi.org/10.1016/j.compositesa.2020.106064
2. Hu H, Zhang F, Luo S, Chang W, Yue J, Wang C (2020) Recent advances in rational design of polymer nanocomposite dielectrics for energy storage. Nano Energy 74:104844. https://doi.org/10.1016/j.nanoen.2020.104844
3. Tu S, Jiang Q, Zhang X, Alshareef HN (2018) Large dielectric constant enhancement in MXene percolative polymer composites. ACS Nano 12(4):3369–3377. https://doi.org/10.1021/acsnano.7b08895
4. Hao Y, Leng Z, Yu C, Xie P, Meng S, Zhou L, Li Y, Liang G, Li X, Liu C (2023) Ultra-lightweight hollow bowl-like carbon as microwave absorber owning broad band and low filler loading. Carbon 212:118156. https://doi.org/10.1016/j.carbon.2023.118156
5. Yin P, Xie P, Tang Q, He Q, Wei S, Fan R, Shi Z (2023) Enhanced dielectric energy storage properties in linear/nonlinear composites with hybrid-core satellite C/SiO_2@TiO_2 nanoparticles. Appl Phys Lett 122(13):132905. https://doi.org/10.1063/5.0143758
6. Li X, Meng S, Xie P, Wei Y, Xu W, Li G, Liang G, Du A, Sun K, Shi Z, Fan R (2023) Two percolation behaviors in binary heterogeneous composites for high permittivity and negative permittivity. Eng Sci 21:795. https://doi.org/10.30919/es8d795
7. Wang C, Zhang Z, Xu X, Wu H, Liu D, Meng S, Li G, Wei Y, Li X, Wang G, Xie P, Liu C (2023) Flexible and biocompatible polystyrene/multi-walled carbon nanotubes films with high permittivity and low loss. ES Mater Manuf 19:791. https://doi.org/10.30919/esmm5f791
8. Behera K, Sivanjineyulu V, Chang Y, Chiu F (2018) Thermal properties, phase morphology and stability of biodegradable PLA/PBSL/HAp composites. Polym Degrad Stab 154:248–260. https://doi.org/10.1016/j.polymdegradstab.2018.06.010
9. Mehboob A, Mehboob H, Chang S (2020) Evaluation of unidirectional BGF/PLA and Mg/PLA biodegradable composites bone plates-scaffolds assembly for critical segmental fractures healing. Compos A 135:105929. https://doi.org/10.1016/j.compositesa.2020.105929
10. Lee S, Kim M, Song HY, Hyun K (2019) Characterization of the effect of clay on morphological evaluations of PLA/biodegradable polymer blends by FT-rheology. Macromolecules 52(20):7904–7919. https://doi.org/10.1021/acs.macromol.9b00800
11. Hou C, Yang W, Kimura H, Xie X, Zhang X, Sun X, Yu Z, Yang X, Zhang Y, Wang B, Xu BB, Sridhar D, Algadi H, Guo Z, Du W (2022) Boosted lithium storage performance by local build-in electric field derived by oxygen vacancies in 3D holey N-doped carbon structure decorated with molybdenum dioxide. J Mater Sci Technol 142:185–195. https://doi.org/10.1016/j.jmst.2022.10.007
12. Jiang X, Chen Y, Meng X, Cao W, Liu C, Huang Q, Naik N, Murugadoss V, Huang M, Guo Z (2022) The impact of electrode with carbon materials on safety performance of lithium-ion batteries: a review. Carbon 191:448–470. https://doi.org/10.1016/j.carbon.2022.02.011
13. Yuan G, Wan T, BaQais A, Mu Y, Cui D, Amin MA, Li X, Xu BB, Zhu X, Algadi H, Li H, Wasnik P, Lu N, Guo Z, Wei H, Cheng B (2023) Boron and fluorine Co-doped laser-induced graphene towards high-performance micro-supercapacitors. Carbon 212:118101. https://doi.org/10.1016/j.carbon.2023.118101
14. Ruan J, Chang Z, Rong H, Alomar TS, Zhu D, AlMasoud N, Liao Y, Zhao R, Zhao X, Li Y, Xu BB, Guo Z, El-Bahy ZM, Li H, Zhang X, Ge S (2023) High-conductivity nickel shells encapsulated wood-derived porous carbon for improved electromagnetic interference shielding. Carbon 213:118208. https://doi.org/10.1016/j.carbon.2023.118208
15. Kang F, Jiang X, Wang Y, Ren J, Xu BB, Gao G, Huang Z, Guo Z (2023) Electron-rich biochar enhanced Z-scheme heterojunctioned bismuth tungstate/bismuth oxyiodide removing tetracycline. Inorg Chem Front 10(20):6045–6057. https://doi.org/10.1039/D3QI01283B
16. Yang L, Li S, Zhou X, Liu J, Li Y, Yang M, Yuan Q, Zhang W (2019) Effects of carbon nanotube on the thermal, mechanical, and electrical properties of PLA/CNT printed parts in the FDM process. Synth Met 253:122–130. https://doi.org/10.1016/j.synthmet.2019.05.008
17. Huang X, Sarmad PM, Dong K, Cui Z, Zhang K, Gonzalez OG, Xiao X (2022) 4D printed TPU/PLA/CNT wave structural composite with intelligent thermal-induced shape memory effect and synergistically enhanced mechanical properties. Compos A 158:106946. https://doi.org/10.1016/j.compositesa.2022.106946

18. Zare Y, Rhee KY (2019) Following the morphological and thermal properties of PLA/PEO blends containing carbon nanotubes (CNTs) during hydrolytic degradation. Compos B 175:107132. https://doi.org/10.1016/j.compositesb.2019.107132
19. Pantano A, Modica G, Cappello F (2008) Multiwalled carbon nanotube reinforced polymer composites. Mater Sci Eng 486(1–2):222–227. https://doi.org/10.1016/j.msea.2007.08.078
20. Raja M, Ryu SH, Shanmugharaj AM (2013) Thermal, mechanical and electroactive shape memory properties of polyurethane (PU)/poly (lactic acid)(PLA)/CNT nanocomposites. Eur Polym J 49(11):3492–3500. https://doi.org/10.1016/j.eurpolymj.2013.08.009
21. Seligra PG, Nuevo F, Lamanna M, Famá L (2013) Covalent grafting of carbon nanotubes to PLA in order to improve compatibility. Compos B 46:61–68. https://doi.org/10.1016/j.compositesb.2012.10.013
22. Sun Y, He C (2013) Synthesis, stereocomplex crystallization, morphology and mechanical property of poly (lactide)–carbon nanotube nanocomposites. RSC Adv 3(7):2219–2226. https://doi.org/10.1039/C2RA23179D
23. Quero E, Müller AJ, Signori F, Coltelli MB, Bronco S (2012) Isothermal cold-crystallization of PLA/PBAT blends with and without the addition of acetyl tributyl citrate. Macromol Chem Phys 213(1):36–48. https://doi.org/10.1002/macp.201100437
24. Ding Y, Feng W, Lu B, Wang P, Wang G, Ji J (2018) PLA-PEG-PLA tri-block copolymers: effective compatibilizers for promotion of the interfacial structure and mechanical properties of PLA/PBAT blends. Polymer 146:179–187. https://doi.org/10.1016/j.polymer.2018.05.037
25. Ahmadzadeh Y, Babaei A, Goudarzi A (2018) Assessment of localization and degradation of ZnO nano-particles in the PLA/PCL biocompatible blend through a comprehensive rheological characterization. Polym Degrad Stab 158:136–147. https://doi.org/10.1016/j.polymdegradstab.2018.10.007
26. Fenni SE, Wang J, Haddaoui N, Favis BD, Müller AJ, Cavallo D (2019) Crystallization and self-nucleation of PLA, PBS and PCL in their immiscible binary and ternary blends. Thermochim Acta 677:117–130. https://doi.org/10.1016/j.tca.2019.03.015
27. Ding Y, Lu B, Wang P, Wang G, Ji J (2018) PLA-PBAT-PLA tri-block copolymers: effective compatibilizers for promotion of the mechanical and rheological properties of PLA/PBAT blends. Polym Degrad Stab 147:41–48. https://doi.org/10.1016/j.polymdegradstab.2017.11.012
28. Wang X, Peng S, Chen H, Yu X, Zhao X (2019) Mechanical properties, rheological behaviors, and phase morphologies of high-toughness PLA/PBAT blends by in-situ reactive compatibilization. COMPOS PART B-ENG 173:107028. https://doi.org/10.1016/j.compositesb.2019.107028
29. Han Y, Shi J, Mao L, Wang Z, Zhang L (2020) Improvement of compatibility and mechanical performances of PLA/PBAT composites with epoxidized soybean oil as compatibilizer. Ind Eng Chem Res 59(50):21779–21790. https://doi.org/10.1021/acs.iecr.0c04285
30. Naikwadi AT, Sharma BK, Bhatt KD, Mahanwar PA (2022) Gamma radiation processed polymeric materials for high performance applications: a review. Front Chem 10:837111. https://doi.org/10.3389/fchem.2022.837111
31. Wang W, Zhang X, Mao Z, Zhao W (2019) Effects of gamma radiation on the impact strength of polypropylene (PP)/high density polyethylene (HDPE) blends. Results Phys 12:2169–2174. https://doi.org/10.1016/j.rinp.2019.02.020
32. Jeon JS, Han DH, Shin BY (2018) Improvements in the rheological properties, impact strength, and the biodegradability of PLA/PCL blend compatibilized by electron-beam irradiation in the presence of a reactive agent. Adv Mater Sci Eng 2018:1–8. https://doi.org/10.1155/2018/5316175
33. Tarawneh MA, Saraireh SA, Chen RS, Ahmad SH, Al-Tarawni MAM, Yu LJ (2021) Gamma irradiation influence on mechanical, thermal and conductivity properties of hybrid carbon nanotubes/montmorillonite nanocomposites. Radiat Phys Chem 179:109168. https://doi.org/10.1016/j.radphyschem.2020.109168
34. Zhou H, Lei H, Wang J, Qi S, Tian G, Wu D (2019) Breaking the mutual restraint between low permittivity and low thermal expansion in polyimide films via a branched crosslink structure. Polymer 162:116–120. https://doi.org/10.1016/j.polymer.2018.12.033
35. Xue S, Wu Y, Liu G, Guo M, Liu Y, Zhang T, Wang Z (2021) Hierarchically reversible crosslinking polymeric hydrogels with highly efficient self-healing, robust mechanical properties, and double-driven shape memory behavior. J Mater Chem A 9:5730–5739. https://doi.org/10.1039/D0TA10850B
36. Trzebiatowska PJ, Echart AS, Correas TC, Eceiza A, Datta J (2018) The changes of crosslink density of polyurethanes synthesised with using recycled component. Chemical structure and mechanical properties investigations. Prog Org Coat 115:41–48. https://doi.org/10.1016/j.porgcoat.2017.11.008
37. Li F, Wu N, Kimura H, Wang Y, Xu BB, Wang D, Li Y, Algadi H, Guo Z, Du W, Hou C (2023) Initiating binary metal oxides microcubes electromagnetic wave absorber toward ultrabroad absorption bandwidth through interfacial and defects modulation. Nano-Micro Lett 15(1):220. https://doi.org/10.1007/s40820-023-01197-0
38. Li T, Wei H, Zhang Y, Wan T, Cui D, Zhao S, Zhang T, Ji Y, Algadi H, Guo Z, Chu L, Cheng B (2023) Sodium alginate reinforced polyacrylamide/xanthan gum double network ionic hydrogels for stress sensing and self-powered wearable device applications. Carbohydr Polym 309:120678. https://doi.org/10.1016/j.carbpol.2023.120678
39. Duan H, Zhuang C, Mei F, Zeng C, Pashameah RA, Huang M, Alzahrani E, Gao J, Han Y, Yu Q, Wang Z (2022) Benzyl (4-fluorophenyl) phenylphosphine oxide-modified epoxy resin with improved flame retardancy and dielectric properties. Adv Compos Hybrid Mater 5(2):776–787. https://doi.org/10.1007/s42114-022-00491-6
40. Gao T, Rong H, Mahmoud KH, Ruan J, El-Bahy SM, Faheim AA, Li Y, Huang M, Nassan MA, Zhao R (2022) Iron/silicon carbide composites with tunable high-frequency magnetic and dielectric properties for potential electromagnetic wave absorption. Adv Compos Hybrid Mater 5(2):1158–1167. https://doi.org/10.1007/s42114-022-00507-1
41. Saif MJ, Naveed M, Asif HM, Akhtar R (2018) Irradiation applications for polymer nano-composites: a state-of-the-art review. J Ind Eng Chem 60:218–236. https://doi.org/10.1016/j.jiec.2017.11.009
42. Ishak KA, Velayutham TS, Annuar MSM, Sirajudeen AAO (2021) Structure-property interpretation of biological polyhydroxyalkanoates with different monomeric composition: Dielectric spectroscopy investigation. Int J Biol Macromol 169:311–320. https://doi.org/10.1016/j.ijbiomac.2020.12.090
43. Mishra S, Sahoo R, Unnikrishnan L, Ramadoss A, Mohanty S, Nayak SK (2021) Enhanced structural and dielectric behaviour of PVDF-PLA binary polymeric blend system. Mater Today Commun 26:101958. https://doi.org/10.1016/j.mtcomm.2020.101958
44. Fan G, Wang Z, Ren H, Liu Y, Fan R (2021) Dielectric dispersion of copper/rutile cermets: dielectric resonance, relaxation, and plasma oscillation. Scr Mater 190:1–6. https://doi.org/10.1016/j.scriptamat.2020.08.027
45. Fan G, Wang Z, Sun K, Liu Y, Fan R (2021) Doped ceramics of indium oxides for negative permittivity materials in MHz-kHz frequency regions. J Mater Sci Technol 61:125–131. https://doi.org/10.1016/j.jmst.2020.06.013
46. Xie P, Zhang Z, Liu K, Qian L, Dang F, Liu Y, Fan R, Wang X, Dou S (2017) C/SiO2 meta-composite: overcoming the λ/a

relationship limitation in metamaterials. Carbon 125:1–8. https://doi.org/10.1016/j.carbon.2017.09.021
47. Guo J, Chen Z, El-Bahy ZM, Liu H, Abo-Dief HM, Abdul W, Abualnaja KM, Alanazi AK, Zhang P, Huang M, Hu G, Zhu J (2022) Tunable negative dielectric properties of magnetic CoFe2O4/graphite-polypyrrole metacomposites. Adv Compos Hybrid Mater 5(2):899–906. https://doi.org/10.1007/s42114-022-00485-4
48. Wu N, Zhao B, Chen X, Hou C, Huang M, Alhadhrami A, Mersal GAM, Ibrahim MM, Tian J (2022) Dielectric properties and electromagnetic simulation of molybdenum disulfide and ferric oxide-modified Ti3C2TX MXene hetero-structure for potential microwave absorption. Adv Compos Hybrid Mater 5(2):1548–1556. https://doi.org/10.1007/s42114-022-00490-7
49. Wang P, Yang L, Gao S, Chen X, Cao T, Wang C, Liu H, Hu X, Wu X, Feng S (2021) Enhanced dielectric properties of high glass transition temperature PDCPD/CNT composites by frontal ring-opening metathesis polymerization. Adv Compos Hybrid Mater 4:639–646. https://doi.org/10.1007/s42114-021-00287-0
50. Bee ST, Qi NOK, Sin LT, Ng HM, Lim JV, Ratnam CT, Ma C (2021) Superior interaction of electron beam irradiation with carbon nanotubes added polyvinyl alcohol composite system. Polymers 13(24):4334. https://doi.org/10.3390/polym13244334
51. Zheng LJ, Li YD, Weng YX, Zhu J, Zeng JB (2019) Localization control of carbon nanotubes in immiscible polymer blends through dynamic vulcanization. Compos B 167:683–689. https://doi.org/10.1016/j.compositesb.2019.03.049
52. Song Y, Zheng Q (2015) Linear rheology of nanofilled polymers. J Rheol 59(1):155–191. https://doi.org/10.1122/1.4903312
53. Li G, Zhao T, Zhu P, He Y, Sun R, Lu D, Wong C (2019) Structure-property relationships between microscopic filler surface chemistry and macroscopic rheological, thermo-mechanical, and adhesive performance of SiO_2 filled nanocomposite underfills. Compos A 118:223–234. https://doi.org/10.1016/j.compositesa.2018.12.008
54. Jiang L, Huang Z, Wang X, Lai M, Zhang Y, Zhou H (2020) Influence of reactive compatibilization on the mechanical, thermal and rheological properties of highly filled PBT/Al2O3 composites. Mater Des 196:109175. https://doi.org/10.1016/j.matdes.2020.109175
55. Yang S, Wu Z, Yang W, Yang M (2008) Thermal and mechanical properties of chemical crosslinked polylactide (PLA). Polym Test 27(8):957–963. https://doi.org/10.1016/j.polymertesting.2008.08.009
56. Zhang B, Clausi M, Heck B, Laurenzi S, M. Santonicola G, Kleperis J, Antuzevičs A, Reiter G, Aleshin AN, Lobach AS (2021) Changes in surface free energy and surface conductivity of carbon nanotube/polyimide nanocomposite films induced by UV irradiation. ACS Appl Mater Interfaces 13(20):24218–24227. https://doi.org/10.1021/acsami.1c02654
57. Urquijo J, Aranburu N, Dagréou S, Guerrica EG, Eguiazábal JI (2017) CNT-induced morphology and its effect on properties in PLA/PBAT-based nanocomposites. Eur Polym J 93:545–555. https://doi.org/10.1016/j.eurpolymj.2017.06.035
58. Ma B, Wang X, He Y, Dong Z, Zhang X, Chen X, Liu T (2021) Effect of poly (lactic acid) crystallization on its mechanical and heat resistance performances. Polymer 212:123280. https://doi.org/10.1016/j.polymer.2020.123280
59. Hu X, Su T, Li P, Li P, Wang Z (2018) Blending modification of PBS/PLA and its enzymatic degradation. Polym Bull 75:533–546. https://doi.org/10.1007/s00289-017-2054-7
60. Hao Y, Tian H, Chen J, Chen Q, Zhang W, Liu W, Liu Y, Chen W, Chen W, Zuo Z, Wang F, Zhang L (2022) Roles of physical filling and chemical crosslinking on the physico-mechanical properties of polylactic acid. J Appl Polym Sci 139(34):52808. https://doi.org/10.1002/app.52808
61. Mazidi MM, Edalat A, Berahman R, Hosseini FS (2018) Highly-toughened polylactide-(PLA-) based ternary blends with significantly enhanced glass transition and melt strength: tailoring the interfacial interactions, phase morphology, and performance. Macromolecules 51(11):4298–4314. https://doi.org/10.1021/acs.macromol.8b00557
62. Meng X, Li Y, AlMasoud N, Wang W, Alomar TS, Li J, Ye X, Algadi H, Seok I, Li H, Xu BB, Lu N, El-Bahy ZM, Guo Z (2023) Compatibilizing and toughening blends of recycled acrylonitrile-butadiene-styrene/recycled high impact polystyrene blends via styrene-butadiene-glycidyl methacrylate terpolymer. Polymer 272:125856. https://doi.org/10.1016/j.polymer.2023.125856
63. Gao F, Liu Y, Jiao C, El-Bahy SM, Shao Q, El-Bahy ZM, Li H, Wasnik P, Algadi H, Xu BB, Wang N, Yuan Y, Guo Z (2023) Fluorine-phosphate copolymerization waterborne acrylic resin coating with enhanced anticorrosive performance. J Polym Sci 61(21):2677–2687. https://doi.org/10.1002/pol.20230108
64. Gong X, Liu Y, Ibrahim MM, Zhang H, Amin MA, Ma Y, Xu BB, Algadi H, Wasnik P, El-Bahy ZM, Guo Z (2023) Activation of inert triethylene tetramine-cured epoxy by sub-critical water decomposition. React Funct Polym 193:105746. https://doi.org/10.1016/j.reactfunctpolym.2023.105746
65. Yan S, Wu G (2022) Thermo-induced chain scission and oxidation of isosorbide-based polycarbonates: degradation mechanism and stabilization strategies. Polym Degrad Stab 202:110028. https://doi.org/10.1016/j.polymdegradstab.2022.110028
66. Jusner P, Schwaiger E, Potthast A, Rosenau T (2021) Thermal stability of cellulose insulation in electrical power transformers–a review. Carbohydr Polym 252:117196. https://doi.org/10.1016/j.carbpol.2020.117196
67. Yamamoto T, Aoki D, Otsuka H (2021) Polystyrene functionalized with diarylacetonitrile for the visualization of mechanoradicals and improved thermal stability. ACS Macro Lett 10(6):744–748. https://doi.org/10.1021/acsmacrolett.1c00352